Arabian Journal of Geosciences (2019) 12: 254
https://doi.org/10.1007/s12517-019-4436-7

ORIGINAL PAPER

Numerical modeling of rigid strip shallow foundations overlaying geosythetics-reinforced loose fine sand deposits

Sameh Abu El-Soud[1] · Adel M. Belal[1]

Received: 25 December 2017 / Accepted: 20 March 2019 / Published online: 29 March 2019

Abstract

This research displays the influence of geogrid inclusions on the bearing capacity of rigid strip shallow foundations overlying sand dunes. An extensive chain of settings—containing plain fill case—is verified by valuing some factors as first geogrid reinforcement depth, vertical spacing between geogrid inclusions, and geogrid extension relative to the footing width on the mobilized bearing capacity. To achieve the research aims, a group of finite element analysis is carried out to assess the studied parameters. For the purpose of validation; two-dimensional plane strain finite element model is implemented completely similar to the previously built experimental model tests using Plaxis code version 8.2. The soil is represented by Mohr-Coulomb soil constitutive model, and the geogrid reinforcement is characterized by tension elastic elements which have only a normal stiffness. Well matching is detected between the physical and numerical model test results. The results designate that geogrid insertion can severely enhance the bearing capacity of rigid strip footing overlaying sand dunes. Additionally, it is revealed that the load-settlement performance can be considerably improved. The effectiveness of the geosynthetics loose fine sand composite increases to the maximum as the optimum values of the assessed parameters are reached.

Keywords Strip footing · Sand dunes · Bearing capacity · Geogrid · Reinforced soil · Numerical model · Experimental model

Introduction

Thousands of years ago, many attempts were performed aiming to improving the soft clay bearing capacity, by adding agricultural fibers as a reinforcement material. In reinforced soil structures, single or multiple layers of a reinforcing material and squeezed soils are located underneath the foundation element to get an intensively improved performance characteristics material. The reinforced earth structure systems are widely used because of the relatively low cost, the easiness of construction, and the convenience of the utilized materials. The reinforced soil techniques are characterized by the raised tension forces and the shear resistance built up by the mobilized frictional resistance at the fill-reinforcement boundaries and passive resistance along the reinforcement transverse members. For a geosynthetic reinforcing material, the major engineering characteristics are tensile strength, tensile modulus, and interface shear strength, as they are resisting the tensile stresses conveyed from the fill material under deformations (Pinto 2002).

The insufficient bearing capacities of the shallow footings due to the improper soil formations cause major defects in foundations and super-structure due to shear strength and settlement considerations (Chao 2006). A solution for this problem could be by using the soil reinforcement systems to enhance the engineering properties of soil (Wu 2003; Chao 2008). Researches in soil reinforcement systems initiated at 1980s, using scale models. As a result of these researches, the reinforced soil with geosynthetics was approved as a good tool to overcome the bearing capacity and settlement problems associated with low quality soil formations (Holtz et al. 1997).

A state-of-the-art article concerning the geosynthetic-reinforced slopes was carried out by Shukla and Sivakugan, 2011, in which analytical, numerical, and experimental models, case studies, and detailed design processes were

Editorial handling: S. K. Shukla

✉ Sameh Abu El-Soud
saelsoud@gmail.com

Adel M. Belal
adel_belal@hotmail.com

[1] Construction and Building Engineering Department, College of Engineering and technology, Arab Academy for Science and Technology and Maritime Transport(AASTMT), Cairo, Egypt

Table 1 List of researches investigated the planer reinforcement inclusions as a soil improving technique

Author	Year	Title	Paper description
Hussein and Meguid 2016	2016	A three-dimensional finite element approach for modeling biaxial geogrid with application to geogrid-reinforced soils	Two-phase 3D numerical modeling is implemented; the first is to model the unconfined biaxial geogrid under tension loading conditions, then applied to solve reinforced soil-stricter interaction problems. The second phase is to study the response of the loaded geogrid-reinforced soil with a square loaded foundation element.
Mosallanezhad et al. 2016	2016	Experimental and numerical studies of the performance of the new reinforcement system under pull-out conditions	Evaluation the performance of (Grid-Anchor) reinforcing system on the mobilized pullout resistance of the proposed composite using both numerical and experimental modeling.
Yu 2015	2015	Influence of choice of FLAC and PLAXIS interface models on reinforced soil–structure interactions	A comparative study in applying finite difference method using $FALC^{3D}$ and finite element method using PLAXIS, in modeling mechanically stabilized earth (MSE), considering the importance of interface between soil and reinforcement.
Zidan 2012	2012	Numerical Study of Behavior of Circular Footing on geogrid-Reinforced Sand Under Static and Dynamic Loading	A chain of axi-symmetry numerical finite element models were performed and analyzed to explore the performance of circular shallow foundations overlaying a reinforced sand under the effect of static and dynamic loading conditions. The modeling of Geogrid was as an elastic element and fill material was simulated using hyperbolic hardening soil constitutive law.
Asakereh 2012	2012	Strip footing behavior on reinforced sand with void subjected to repeated loading	A series of experimental model tests on strip shallow foundations were performed on unreinforced and geogrid-reinforced sand with an inside void. The footing is under the effect of both static and dynamic loads.
Sao-Jeng Chao 2009	2009	Improving Bearing Capacity of Shallow Foundations on Weak Soils Utilizing Geosynthetic Reinforcing Technique	A summary is made for the procedures of the theoretical progress, laboratory models work, and numerical modeling on the bearing capacities of footings overlaying reinforced soils utilizing the geosynthetic reinforcing technique.
Alamshahi and Hataf 2009	2009	Bearing capacity of strip footings on sand slopes reinforced with geogrid and grid-anchor	This research offering the influence of a different form of geogrid inclusion on the bearing capacity of a rigid strip shallow foundations overlaying a sand slope.
Madhavi and Somwanshi 2009	2009	Effect of reinforcement form on the bearing capacity of square footings on sand	The output of an experimental and numerical model tests for square footing overlaying a geosynthetic-reinforced sand formation are presented, with comparing the gained enactment of different geosynthetic forms using the same quantity of each.
Sharma et al. 2009	2009	Analytical modeling of geogrid reinforced soil foundation	An analytical modeling methodology is developed for valuing the ultimate bearing capacity of (geogrid-reinforced soil foundations (GRSF)) for different soil types.
Ghazavi and Lavasan 2008	2008	Interference effect of shallow foundations constructed on sand reinforced with geosynthetics	This research inspects using numerical modeling, the bearing capacity ratio (BCR) for rough square shallow foundations overlaying a Geogrid-reinforced sandy soil deposits.
El Sawwaf 2007	2007	Behavior of strip footing on geogrid-reinforced sand over a soft clay slope	The possible aids of using replacement with a reinforced sand layer made adjacent to a slope crest was considered. A chain of two-dimensional plain strain finite element analyses (FEA—using PLAXIS—was done on a physical slope model.
Basudhar et al. 2007	2007	Circular footings resting on geotextile-reinforced sand bed	Prediction the load-settlement characteristics using both analytical and numerical modeling those compared with a physical laboratory model output.
Al-Sinaidi and Ali 2006	2006	Improvement in bearing capacity of soil by geogrid in experimental approach.	An effort is paid to present the particulars of the study of behavior of geogrids and soil composite. For this objective, a single footing model tests were carried out for soil with and without multi-layers of geogrid at changed reinforcement burial depth. The (load- settlement) behavior was traced for all reinforcement arrangements.
Patra et al. 2005	2005	Eccentrically loaded strip foundation on geogrid-reinforced sand	Valuing the ultimate bearing capacity by using physical laboratory model tests for the case of eccentrically loaded strip footing overlaying a geogrid-reinforced sand. An empirical relations has been submitted that relates both cases of reinforced and unreinforced soils.

Table 1 (continued)

Author	Year	Title	Paper description
Ghosh and Bera 2005	2005	Bearing capacity of square footing on pond ash reinforced with jute-geotextile	For the mitigation of the environmental dangers related to disposal areas of pond ash, it has been employed as a treated controlled fill to improve the bearing capacity of the proposed site condition by adding a natural tension fibers named jute as a foundation layer below the tested square footing.
Boushehrian and Hataf 2003	2003	Experimental and numeri-cal investigation of the bearing capacity of model circular and ring footings on reinforced sand	This research is carried out using experimental and numerical model tests on circular and ring shallow foundation elements to inspect the bearing capacity of geosynthetic-reinforced sand.
Yetimoglu et al. 1994	1994	Bearing capacity of rectangular footings on geogrid-reinforced sand	A research was conducted to explore the bearing capacity of rectangular shallow foundation overlaying a geogrid-reinforced sandy deposit by mean of both numerical and experimental models.
Omar et al. 1993	1993	Ultimate bearing capacity of shallow foundations on sand with geogrid reinforcement	Evaluation and analysis of the attained bearing capacity ratio (BCR) of strip and square footings overlaying a geogrid-reinforced sandy deposits throughout an experimental model tests.
Khing et al. 1993	1993	The bearing-capacity of a strip foundation on geogrid-reinforced sand	An experimental model for strip footing overlaying a geogrid-multi-layer reinforced sand is carried out. Results of enhancement in bearing capacity are presented relative to the ultimate bearing capacity at a limited settlement levels for the foundation element.
Guido et al. 1986	1986	Comparison of geogrid and geotextile reinforced earth slabs	A comparison was presented for the outcomes of physical model tests implemented to evaluate the bearing capacity and pullout resistance of earth slabs treated with geosynthetics.
Fragaszy and Lawton 1984	1984	Bearing Capacity of Reinforced Sand Subgrades	Experimental strip footing model tests were carried out on both geosynthetics—improved and unimproved sand soils. Test results were compared with that of an analytical-based prediction for reinforced sand bearing capacity. The research highlighted the surface roughness of the reinforcement material as an important factor.
Akinmusuru and Akinbolade 1981	1981	Stability of loaded footings on reinforced soil	Presentation of the mobilized bearing capacity of experimental scale model tests for case of 100 mm^2 footing overlaying a rope fiber-reinforced sand deposit.

reported. Nevertheless, more investigations were conducted for more understanding of the advantages of using planar reinforcement inclusions in soil improvement as tabulated in Table 1.

Tests on geosynthetic-reinforced clay showed a raise in limit loads (Sakti and Das 1987). Adams and Collin 1997 confirmed the benefit of geosynthetic reinforcement for soil using a large-scale laboratory model tests on square footings. A primary estimation of limit loads on soils improved by geosynthetics as foundation strata was tried in the area of unpaved roads (Giroud and Noiray 1981).

A numerical investigation related to the optimal burial depth of the reinforcement within sand formations was done by Aria et al. 2017. The study concluded that the optimum burial depth depends significantly on the angle of internal friction (ϕ) of sand. For any value of (ϕ), there are two optimal burial depths: the first is constant depth equals 0.2 times the foundation width (B), which is mostly possessing the maximum improvement in bearing capacity, and the second is optimal burial depth which ranges between 0.38B and 0.5B as (ϕ) increases from 25 to 30°.

Table 2 Soil parameters used in FEM

Unit weight	17.78 kN/m^3
Young's modulus [E_{ref}]	25,000 kN/m^2
Poisson ratio [$\nu_{(nu)}$]	0.35
Cohesion [C_{ref}]	15 kN/m^2
Friction angle [ϕ]	30°
Dilatancy angle [Ψ]	0°

Table 3 Geogrid parameters used in FEM

EA	500 kN/m
Np	45 kN/m

Table 4 Strip footings—steel model and R.C. real full scale dimensions

Steel model footings (m)	
A	0.075
B	0.1
C	0.12
Full scale R.C. footings (m)	
D	1
H	3
L	5

Investigations for the geocell reinforcement were carried out by Hegde and Sitharam 2015 through the implementation of a 3D numerical modeling for geocell and geogrid using finite difference package FALC^{3D}. The model was validated with experimental studies, and then was used in the evaluation of geocell properties on the performance of the reinforced foundation beds.

A hypothetical mechanical models were carried out by Shukla and Chandra, 1994a, b, in which they presented a generalized model to assess the settlement characteristics of the reinforced granular fill overlaying soft soil formation. They concluded that:

- The compressibility of the granular fill has an appreciable influence on the settlement response of the system, as long as the granular fill stiffness is less 50 times than that of the soft formation.
- The granular fill compressibility increase results in more settlement at the edge of the loaded area.
- At higher load intensities; the reinforced granular fill-soft soil system behaves as much stiffer system.

The improvement of shallow foundations performance using reinforced soil techniques was studied and it was revealed that the improved soil with geogrid insertion is one of the most economic modifications for insufficient soil conditions. The enhancement gained by using geosynthetics is highly related to its usage form.

Table 5 Model steel plate footing parameters used in the FEM

Plate properties			
Unit weight (γ_{Steel})	78.4	kN/m^3	
Modulus of elasticity (E)	2E+08	kN/m^2	
Thickness in (cm)	1	1	1
Width in (cm)	7.5	10	12.5
EA—axial stiffness (kN/m)	150,000	200,000	250,000
EI—bending stiffness (kN m^2/m)	1.25	1.6667	2.0833
Own weight (kN/m/m)	0.0588	0.0784	0.098

Table 6 Real concrete footing parameters used in the FEM

Material model	Linear elastic
Unit weight (γ_{RC})	23.563 kN/m^3
Young's modulus [E_{ref}]	2.482E+07 kN/m^2
Poisson ratio [$v_{(nu)}$]	0.25

This research is presenting outcomes of the proposed numerical model and the previously studied experimental model tests in addition to analysis for a rigid strip footing founded on reinforced dune sand bed. The current investigation is conducted to suggest the soil reinforcement system using geogrids as an efficient alternate to solve the technical problems associated with shallow foundations rested on weak soils.

Finite element modeling

Two-dimensional finite element code (PLAXIS) was employed for more knowledge about the behavior of the reinforced soil with geogrid beneath a rigid shallow foundations. The Mohr-Coulomb constitutive model is used for fill material and elastic tensile model for geogrid reinforcement to envisage the bearing capacities and settlements characteristics. The assigned materials for all of the model individuals, namely, fill geogrid, strip footing, and interface elements, were defined

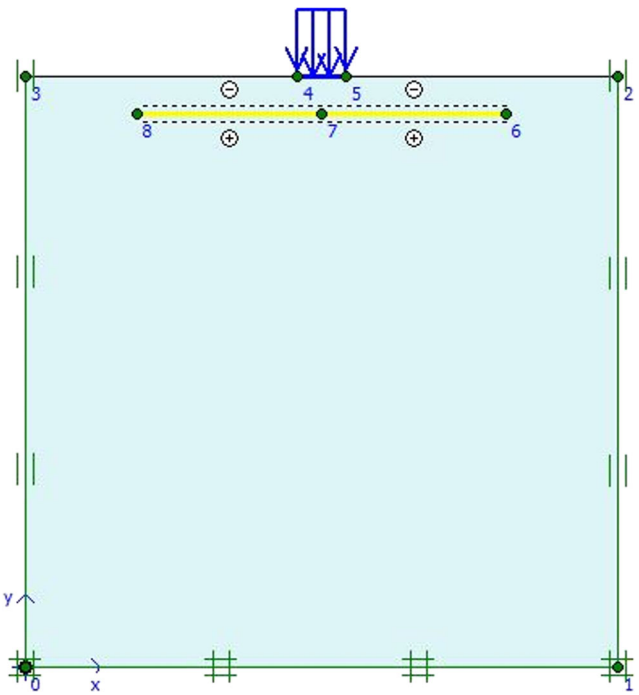

Fig. 1 Finite element model—geometry, vertical load, and boundary conditions

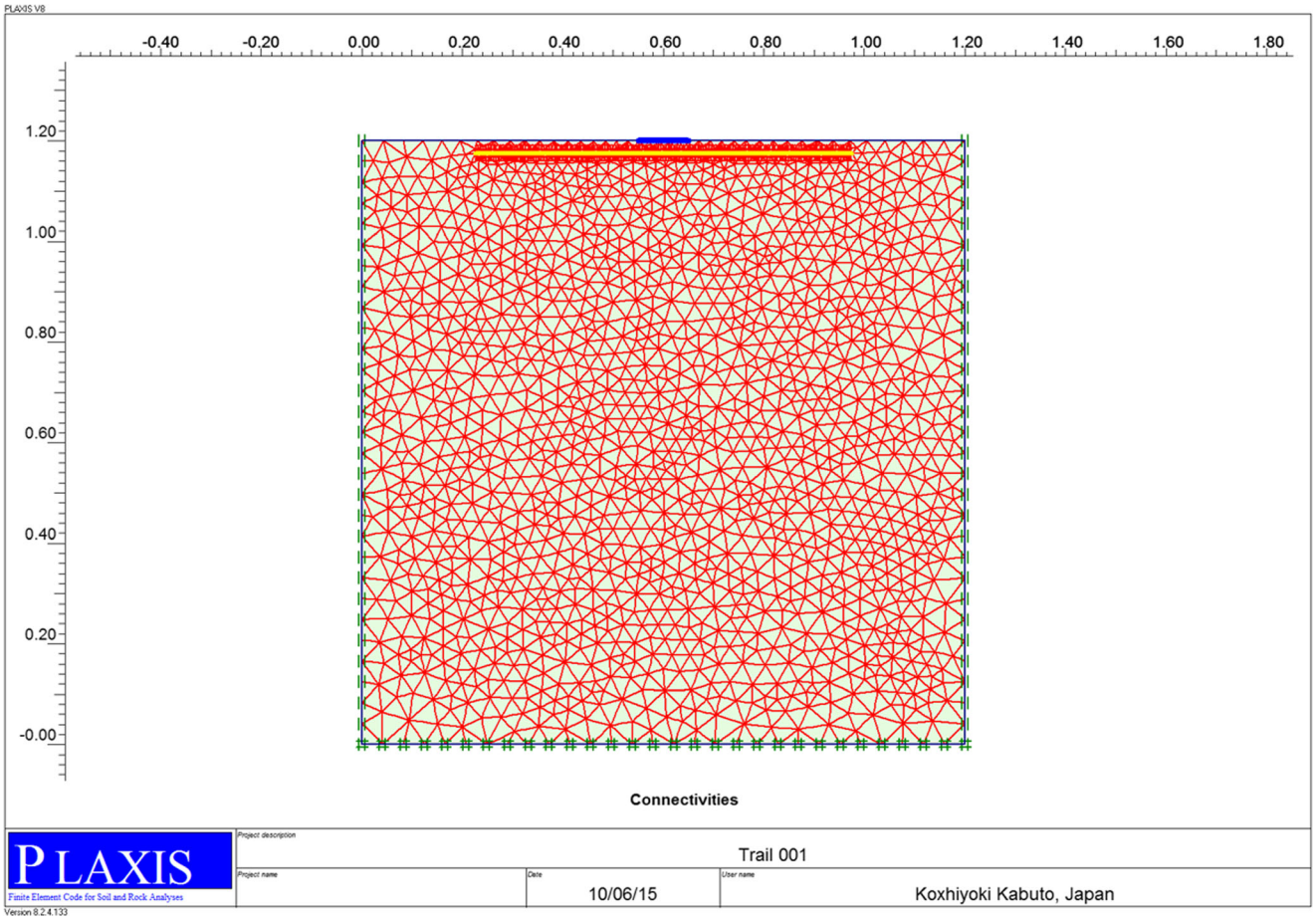

Fig. 2 Finite element model—un-deformed mesh

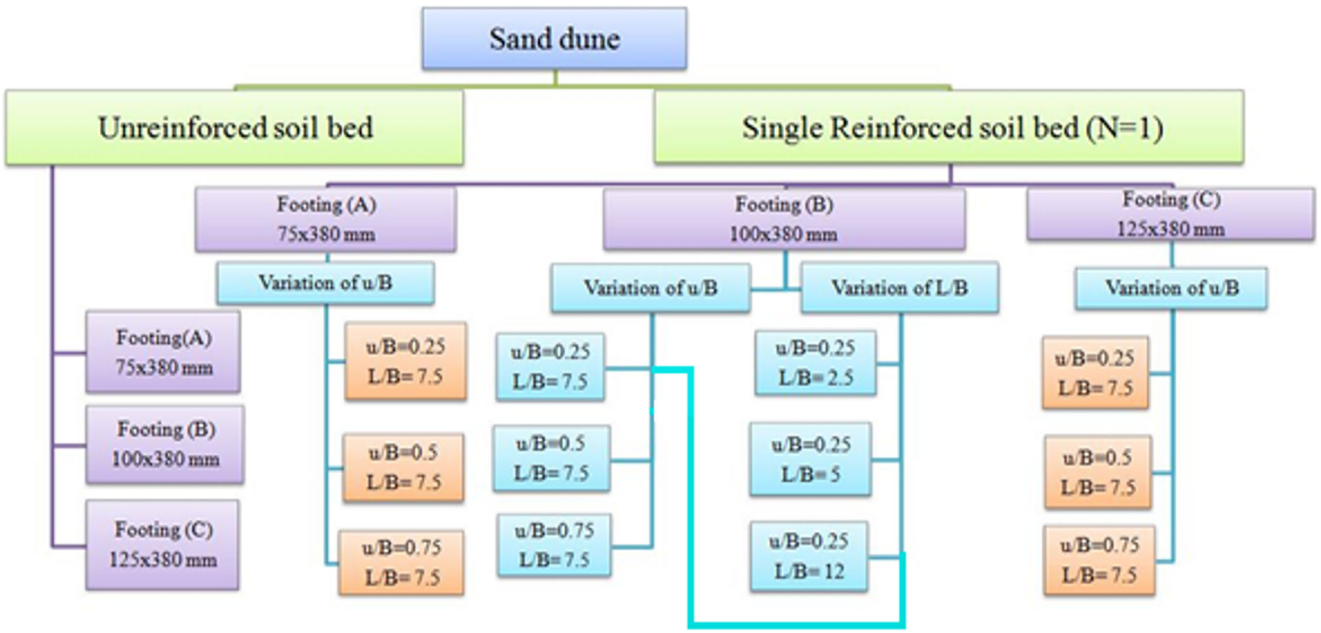

Fig. 3 FEM matrix for single-layer reinforced soil bed

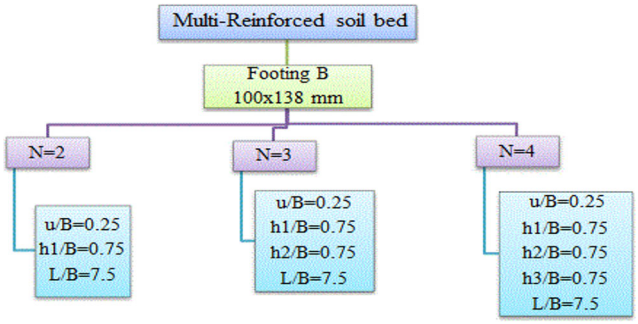

Fig. 4 Previous experimental testing program matrix for multi-reinforced soil bed

with the proposed boundary conditions and loading system as described herein.

A chain of two-dimensional finite element models for fine sand-geogrid-strip footing system was implemented to simulate the obtained experimental model tests, to define the deformations pattern in the sandy fill body, and to validate the numerical model. The used 2D finite element code supports mesh construction using triangular elements of six or 15 nodes for each element of the simulated fill material.

Material modeling

Soil constitutive law

The recognized Mohr-Coulomb constitutive law was used as a first-order (linear) simulation of actual soil performance. This elasto-plastic, stress-strain relation involves five elementary input parameters: the dry and wet fill unit weight, Young's modulus [E_{ref}], Poisson ratio [v_{nu}], cohesion [C_{ref}], friction angle [ϕ], and the dilatancy angle [Ψ]. The values of these parameters were determined through the laboratory testing program for the used fill and are presented in Table 2.

Geogrid modeling

Geogrid is an elastic flexible element with only normal stiffness that can only withstand tensile forces. The geogrid

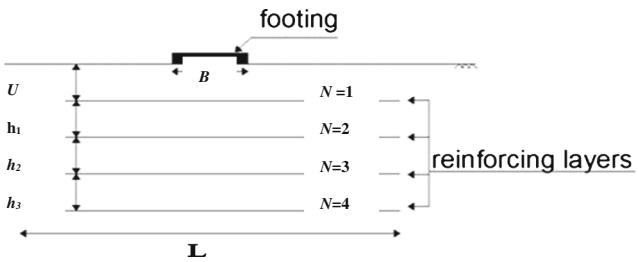

Fig. 5 Geogrid reinforcement layout

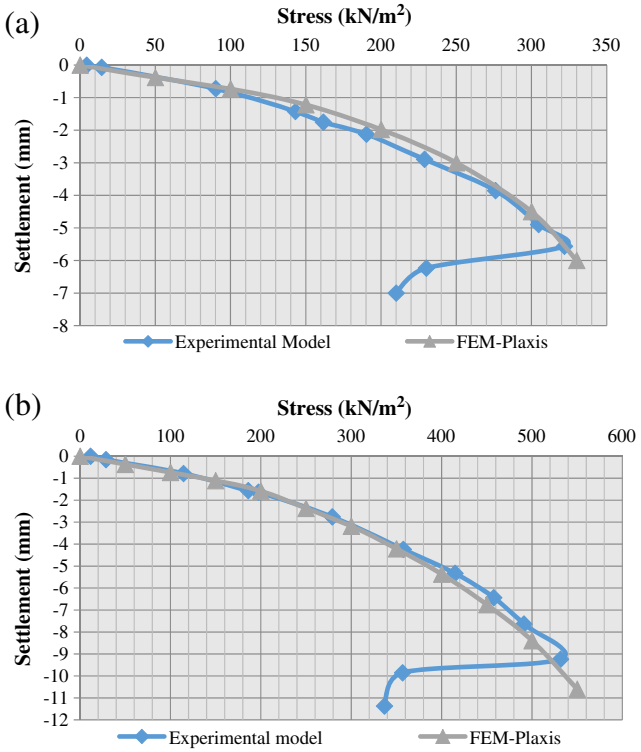

Fig. 6 Relationship between bearing stress and vertical displacement for footing type (B) on **a** unreinforced soil bed and **b** single reinforced soil bed

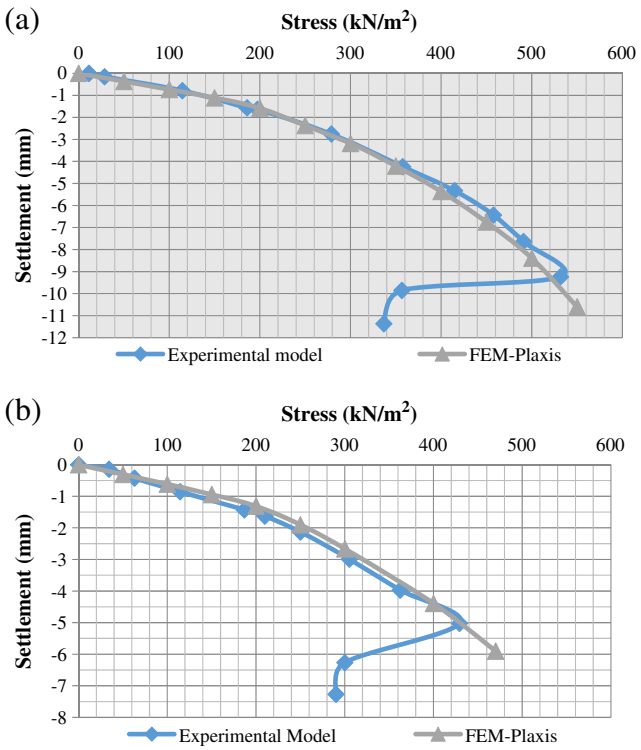

Fig. 7 Effect of first geogrid embedment (u/B) on bearing stress–footing vertical displacement relationship for footing type (B) on single-reinforced soil bed for $N = 1$, $L/B = 7$: **a** $u/B = 0.25$ and **b** $u/B = 0.5$

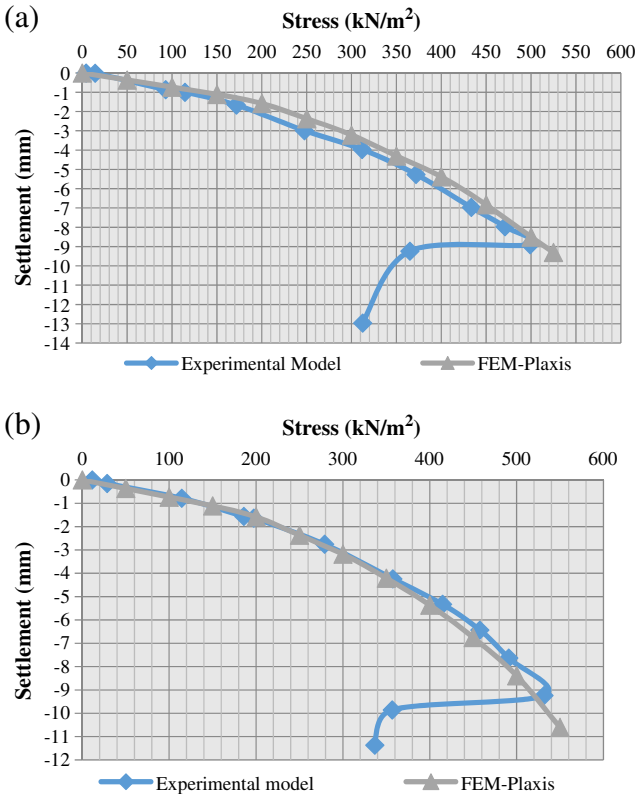

Fig. 8 Effect of geogrid extension (L/B) on bearing stress–footing vertical displacement relationship for footing type (B) on single-reinforced soil bed for $N = 1$ and $u/B = 0.25$: **a** $L/B = 5$ and **b** $L/B = 7$

was modeled using elastic tensile constitutive model as that available in Plaxis code Version 8.2, with the parameters determined using the universal axial tension machine as shown in Table 3, where (EA) represents axial/normal stiffness and (N_p) represents the geogrid ultimate tensile strength.

Strip footing modeling

Six strip footings (A), (B), (C), (D), (H), and (L) were modeled with the dimensions shown in Table 4.

The steel strip footings (A), (B), and (C) were modeled as a plate with the steel parameters shown in Table 5; however, the reinforced concrete strip footings (D), (H), and (L) were modeled as a reinforced concrete element with proper interface properties. All footings input parameters were presented in Table 6.

Interface elements

The roughness of the interface elements (contact surfaces between fill material and geogrid reinforcement) were represented by selecting a proper value for the reduction factor of the shear strength at the interface (R_{inner}). This factor relates the interface element shear characteristics as a percentage of the fill shear strength parameters (friction angle and cohesion). In this model, the interface element between the soil and the geogrid had the typical value of $R_{inner} = 0.85$. The interface element between the soil and the steel plate was chosen as rigid interface ($R_{inner} = 1$), and between the concrete footing and the soil was chosen with the typical value of $R_{inner} = 0.6$. The values of the R_{inner} were chosen based on the previous experience with the interaction between soils and geogrids which develop bearing and friction stresses.

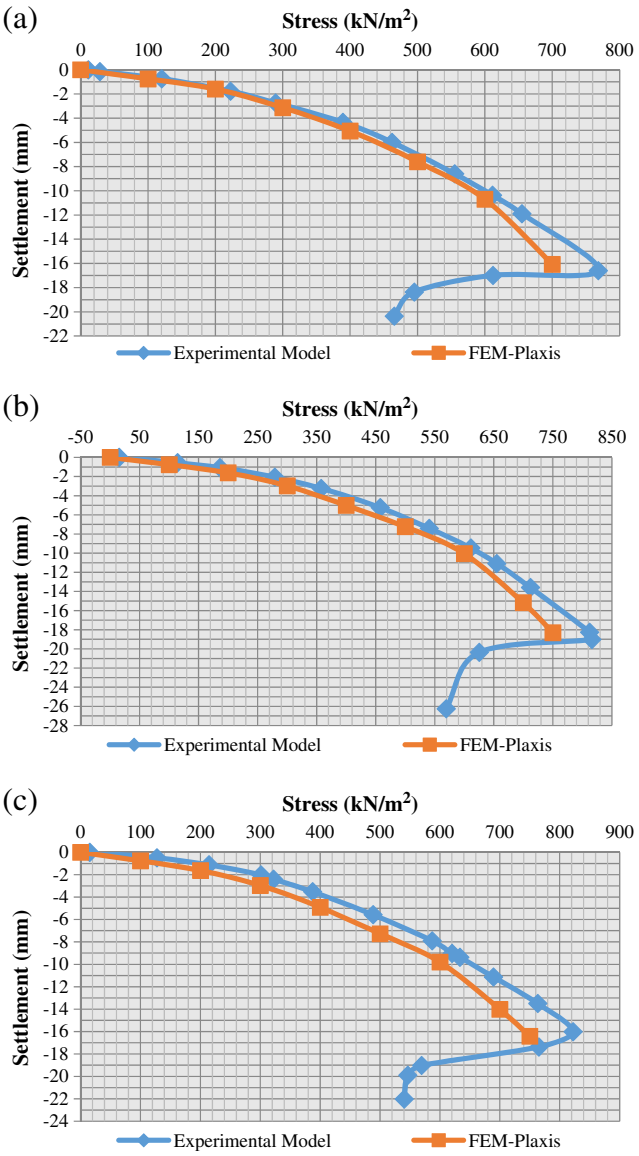

Fig. 9 Effect of number of geogrid layers (N) on bearing stress–footing vertical displacement relationship for footing type (B) on multi-reinforced soil bed for $u/B = 0.25$ and $L/B = 7$: **a** $N = 2$, $h1/B = 0.75$, **b** $N = 3$, $h1/B = h2/B = 0.75$, and **c** $N = 4$, $h1/B = h2/B = h3/B = 0.75$

Boundary conditions and vertical load on the strip footing

The demonstrated boundary conditions were constructed such that the boundaries of both model sides were free vertically and constrained horizontally, while the bottom horizontal boundary was fully fixed to simulate the fill particle movements in all directions as in the physical model as shown in Fig. 1. The load on the strip footing was simulated by employing an incremental pre-described load (load control method) that was associated with a multi-step loading procedure up to failure.

Mesh generation and initial conditions

Once the model geometry was defined, the material properties were assigned to all clusters (different zones in the generated mesh elements including certain number of finite elements) and the structural objects were defined. The geometry inputs have to be divided into elements as shown in un-deformed mesh in Fig. 2 to perform finite element calculations. A refined mesh (more elements with smaller dimensions) was implemented to reduce the effect of mesh dependency for cases involving variations in the reinforcement layers: number, length, and location relative to the footing. Then, the initial stress condition was conducted by applying the gravity force due to soil own weight with the existence of geogrid reinforcements. The initial conditions included the initial groundwater circumstances, the initial geometry alignment, and the initial effective stress state.

Finite element modeling matrix

A chain of two-dimensional numerical models were implemented and analyzed for achieving the research aim. Figures 3 and 4 show the FEM matrices for the single- and multi-layered reinforcement cases, which is the same matrix carried out for the previous conducted experimental testing program. In the multi-layered case, the FEM was made on footing type (B) (refer to Table 5) for $h/B = 0.75$. Figure 5 shows the geogrid layout and terms definition, where (N) is the geogrid inclusions number, (L) is the geogrid extension length relative to the footing width, (u) is the embedment of the first geogrid layer measured from bottom of the strip

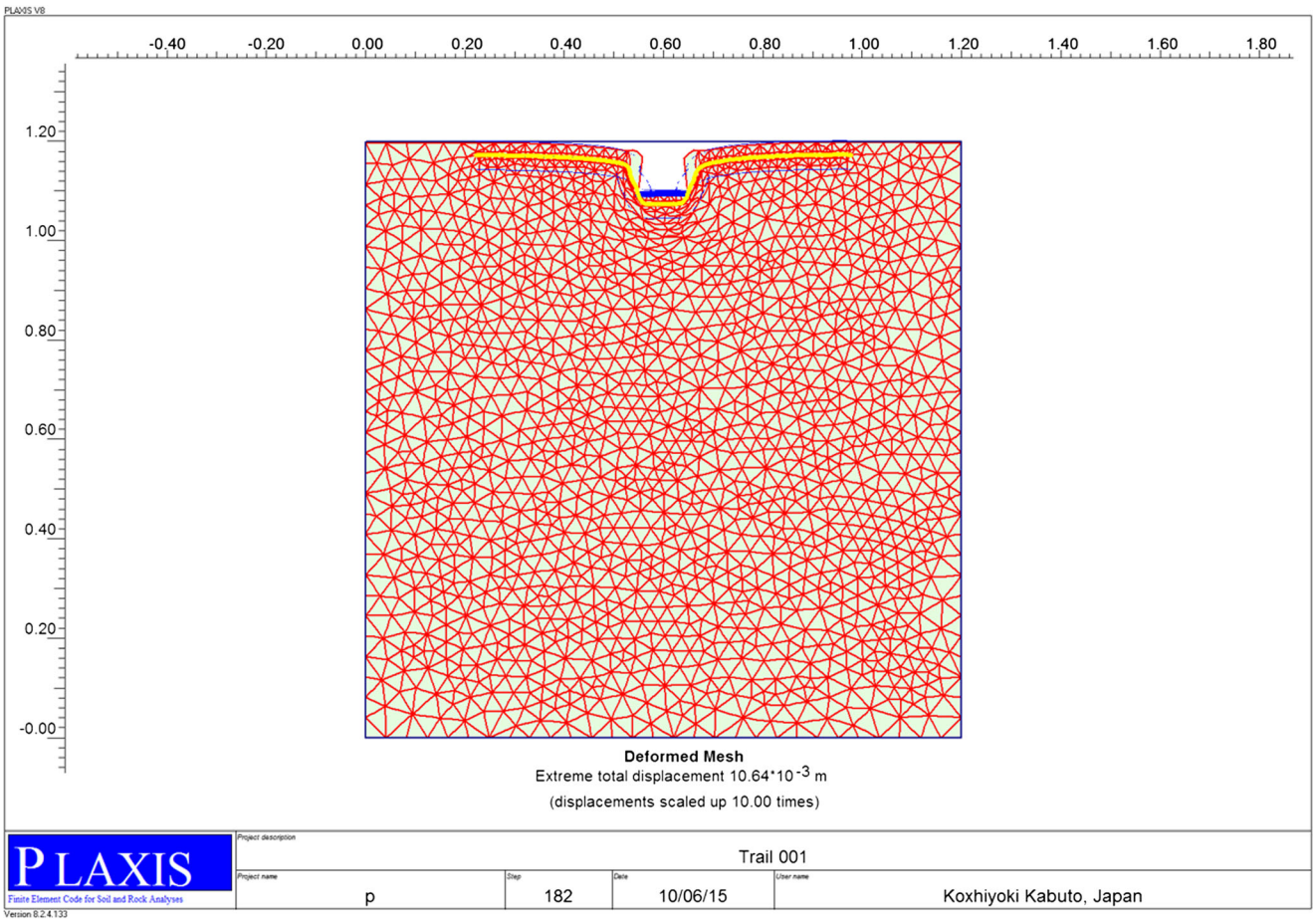

Fig. 10 Finite element model—deformed mesh

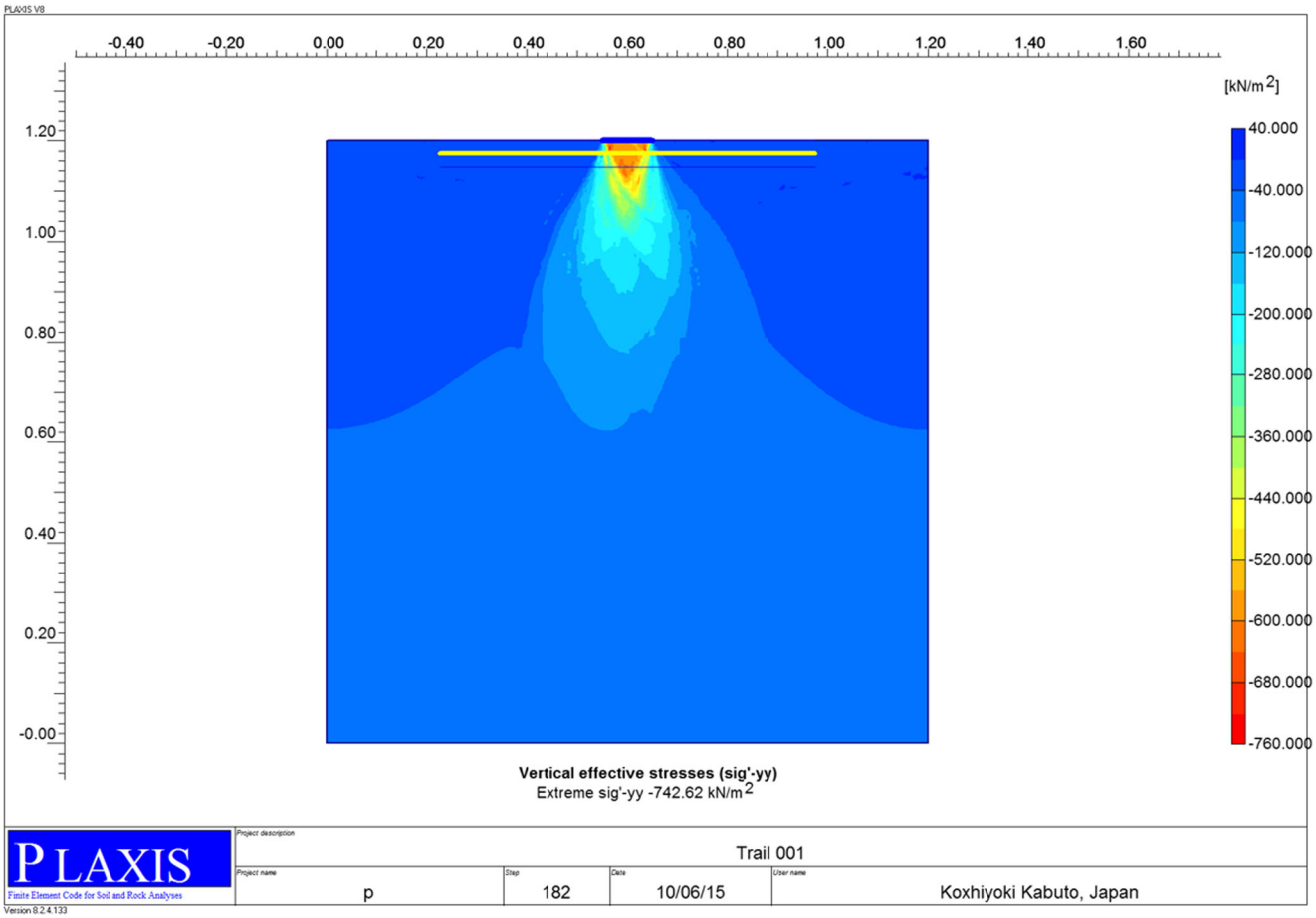

Fig. 11 Effective vertical stresses contours (Sig_{yy})

footing, (h) is the vertical spacing between consecutive layers of the geogrid, and (B) is the footing width.

Validation of finite element model

To validate the proposed numerical model, the geometry and materials of the geogrid-soil-strip footing system were made to be completely similar to the experimental model and included steel strip footing, geogrid, and sandy fill. The results are presented in Figs. 6, 7, and 8 in terms of stress under the footing in (kN/m^2) vs settlement in (mm) for unreinforced, single-reinforced, and multi-reinforced soil beds. All results are presented for finite element model (FEM) versus previously studied experimental model for comparison and validation.

Unreinforced soil bed

Stress–settlement relationship of the rigid strip footing resting on unreinforced sand dunes was produced for both experimental and numerical models to be reference tests. Figure 6 a illustrates the comparison between FEM and the experimental model results for footing (B) on unreinforced soil bed.

Single-reinforced soil bed for footing type (B)

To examine the influence of the single-reinforcement burial depth (u/B) and the extension of the reinforcement relative to the footing width (L/B), these two parameters were studied using the proposed numerical model and were compared with the results of the previously constructed experimental model for the validation purpose as shown in Figure 6b.

Effect of u/B for footing (B)

The embedment ratio (u/b) was investigated as a variable with all of the other parameters influencing the soil-geogrid-strip footing system were kept fixed. Figure 7 a and b illustrate the comparison between the proposed FEM and the previous experimental model results for footing (B) with $N = 1$, $L/B = 7.5$ and $u/B = 0.25$ and 0.5 respectively.

Effect of L/B with footing (B)

As previously known that the bearing capacity ratio (BCR) rises as the reinforcement inclusion length spreads further than the failure pattern under the footing, the reinforcement

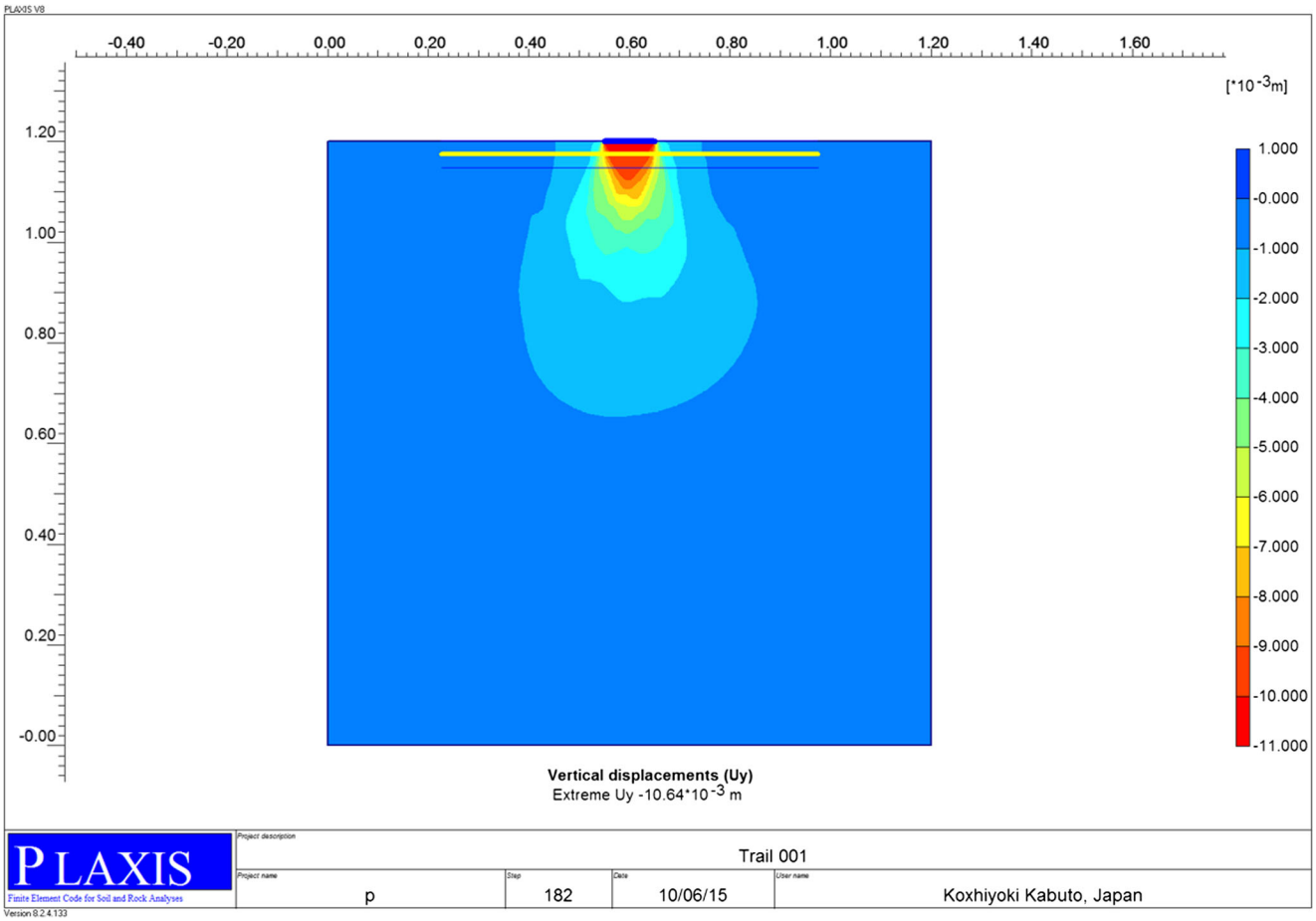

Fig. 12 Vertical displacements contours (U_y)

length is the major parameter governing the (BCR). Figure 8 a and b illustrate the comparison between the proposed FEM and the previously obtained experimental model test results of bearing stress versus strip footing settlement for footing (B) with $N = 1$, $u/B = 0.25$, and $L/B = 5$ and 7 respectively.

As described in the above Figs. 6, 7, and 8 in the FEM validation process, the test results of the single-layer reinforced soil bed and the comparison indicated that there is a considerable matching for the experimental model and FEM results which is accepted.

Multi-reinforced soil bed

Figure 9 a, b, and c illustrate the comparison between the proposed FEM and the previously obtained experimental results for footing (B) with $L/B = 7.5$, $u/B = 0.25$, and $h1/B = h2/B = h3/B = 0.75$ for $N = 2$, 3, and 4 respectively.

It can be noticed by relating the finite element model and the previous physical model results for the cases of unreinforced, single-reinforced, and multi-reinforced soil beds that there is a considerable matching for the FEM and the experimental model results. Therefore, the FEM is validated and ready for the parametric study.

Finite element model outputs

A sample of the finite element model outputs was presented for only one of the assessed configurations. These outputs included effective stresses within the tested soil under the footing, the soil elements that reaches the plastic state, horizontal and vertical displacements within soil mass and in geogrid reinforcement, and tension force distribution in geogrid. Figures 10, 11, 12, 13, and 14 show these outputs for the case of $N = 1$, $u/B = 0.25$, and $L/B = 7.5$ for footing (B).

Results, analysis, and discussion

The analysis was carried out for both single and multi-reinforced soil model test results and was presented through the bearing capacity ratio (BCR). This factor is expressed as the percentage of the footing ultimate pressure with reinforced foundation (q reinforced) to that for unreinforced bed (q_{un} unreinforced).

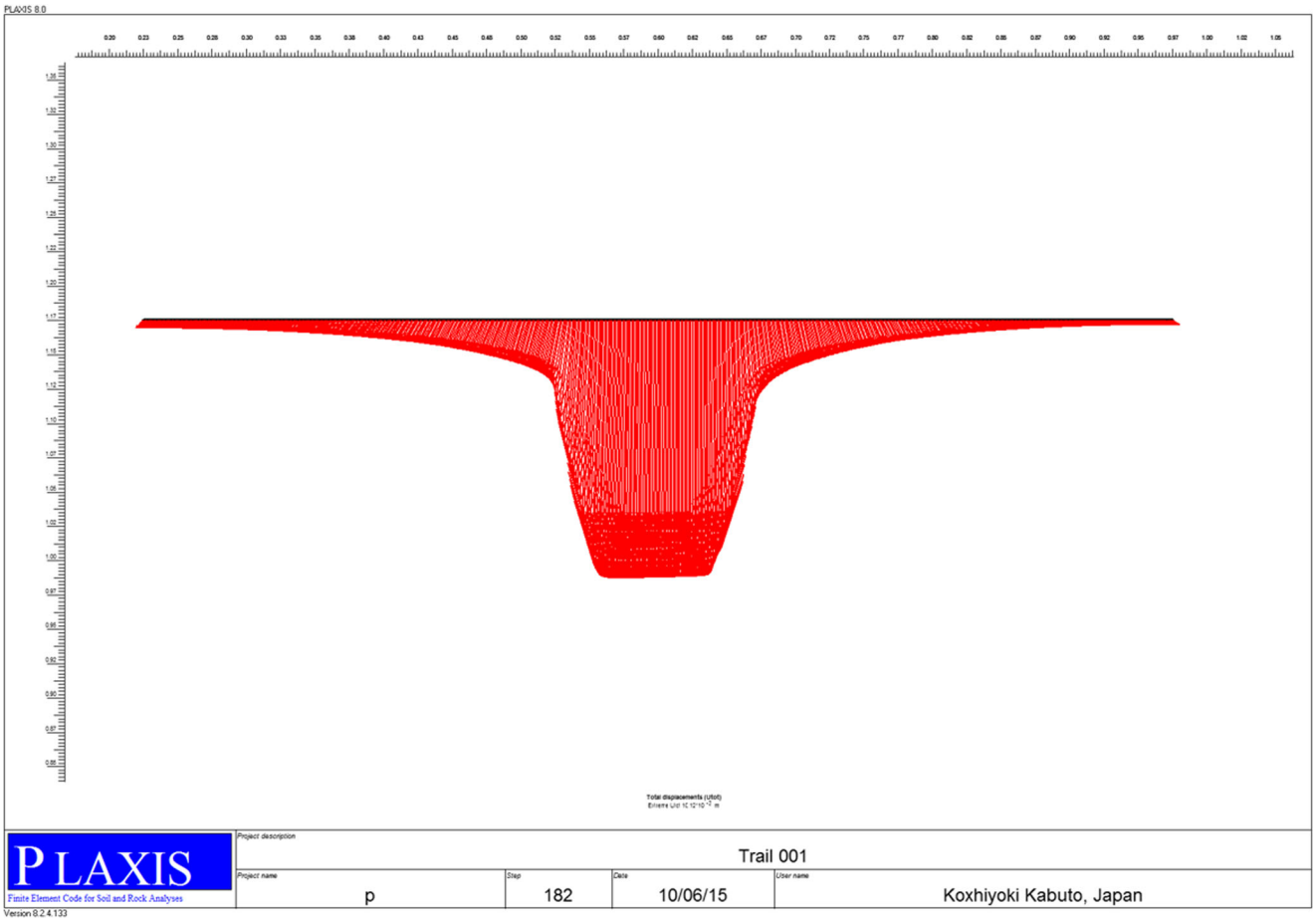

Fig. 13 Geogrid reinforcement total displacements (U_{lot})

Single reinforcement soil bed

Effect of first reinforcing layer depth (u/B)

The depth of the first reinforcing layer was changed in terms of $u/B = 0.25$, 0.5, and 0.75 for $L/B = 7.5$ for footings (A), (B), (C), (D), (H), and (L) (refer to Table 3) to get the optimum embedment depth. Figure 15 displays the variation of the bearing capacity ratio (BCR) of the soil versus the assessed parameter u/B. It was noticed that the (BCR) values for $u/B = 0.25$ and $L/B = 7.5$ were 1.67, 1.67, 1.63, 1.18, 1.10, and 1.07, respectively, with footings changed from (A) to (L) which indicate an improvement of 67 to 7% respectively. That means that as the width of the footing decreases, the improvement in terms of *BCR* increases with an optimum value at $u/b = 0.25$

Effect of reinforcing layers width (*L/B*)

The geogrid layer width relative to the strip footing width was changed in terms of $L/B = 2.5$, 5, 7.5, and 12 for $u/B = 0.25$ for footings (B), (D), (H), and (L) to get the optimum width for the maximum (BCR). Figure 16 illustrates the (BCR) of the soil versus the assessed parameter L/B.

It can be noticed that the effect of using $L/B = 7.5$ and 12 was almost the same; therefore, the optimum value of the parameter $L/B = 7.5$ for all tested footings. Also, It can be noticed that the values of (BCR) for $L/B = 7.5$ and $u/B = 0.25$ were 1.6, 1.13, 1.10, and 1.07 for footings (B), (D), (H), and (L), respectively. This means that as the width of the reinforcement increases, the improvement of the BCR increases up to $L/B = 7.5$ and as the width of the footing decreases the improvement of the BCR increases.

Multi-reinforcement soil bed

Effect of the spacing between the first and second geogrid (*h1/B*)

For the case of using two reinforcing layers with $u/B = 0.25$, $L/B = 7.5$, and $h1/B = 0.75$, the inspection of the results in Fig. 17 revealed that the values of (BCR) were 2.5, 2.12, 1.85, 1.32, 1.20, and 1.14 for footings (A), (B), (C), (D), (H), and (L), respectively. This indicates an inverse proportion between footing width (B) and the improvement in the *BCR* that ranges between 14 and 150% with the ($h1/b$) optimum value = 0.75 for all of the tested footings.

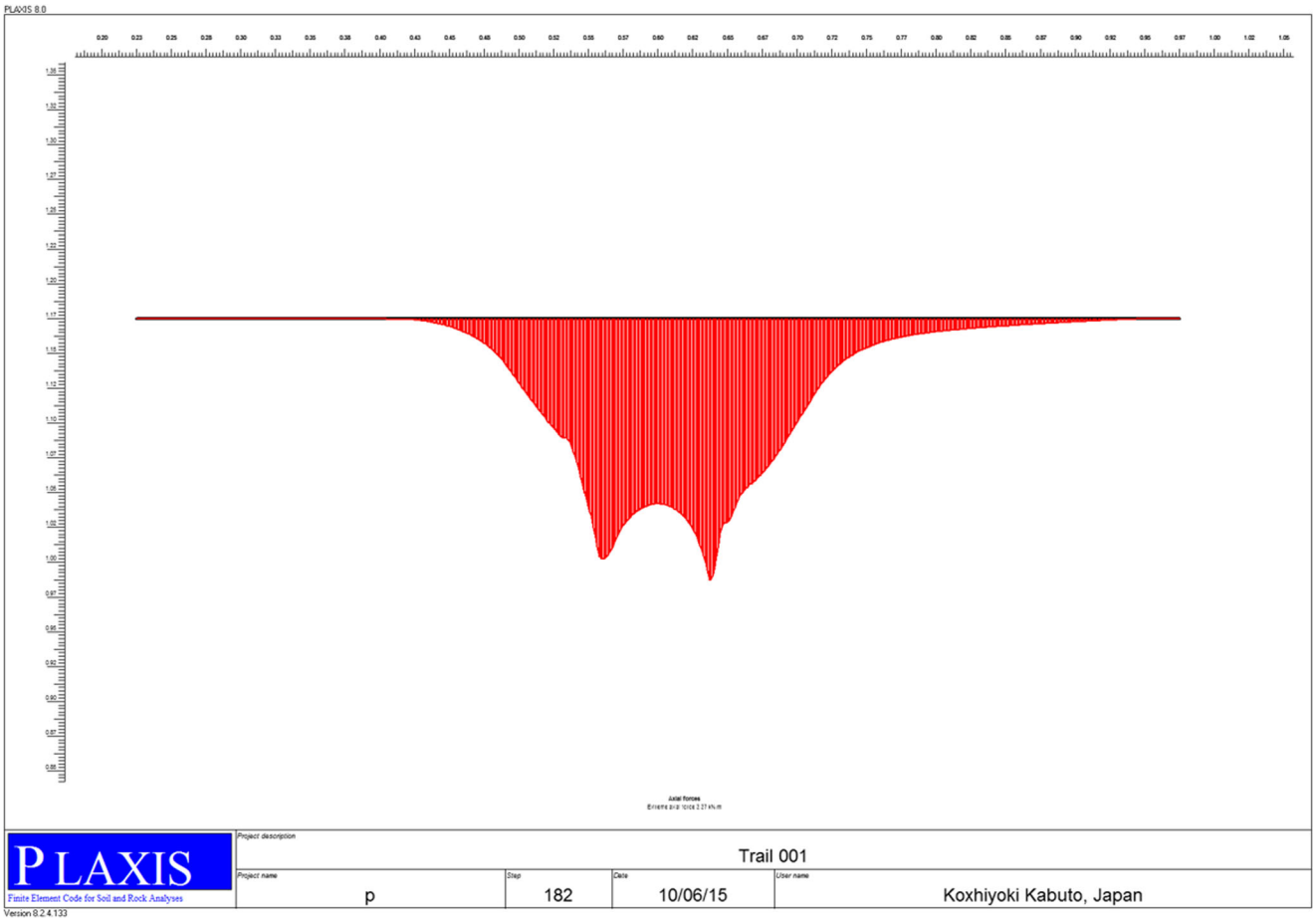

Fig. 14 Geogrid reinforcement axial forces

Effect of the spacing between the second and third geogrid (h_2/B)

Bearing capacity ratio (BCR) In this part, the results were analyzed and discussed for the case of using three geogrid reinforcement layer, with fixing the spacing between the first and the second layers (h_1/B) and varying the spacing between the second and the third layers (h_2/B) to be assessed. From Fig. 18, it can be noticed that the values of (BCR) for using three reinforcing layers with $u/B = 0.25$, $L/B = 7.5$, and $h_1/B = 0.75$, $h_2/B = 0.75$ were 2.5, 2.27, 2.14, 1.36, 1.3, and 1.25 for footings (A), (B), (C), (D), (H), and (L), respectively. This indicates an inverse

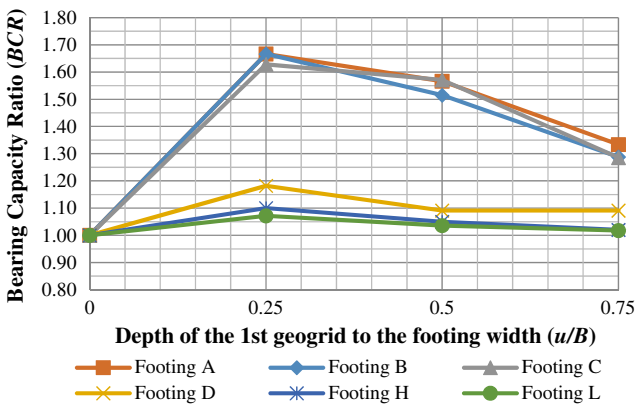

Fig. 15 Relationship of bearing capacity ratio BCR vs first geogrid embedment (u/B) for footings (A), (B), (C), (D), (H), and (L)

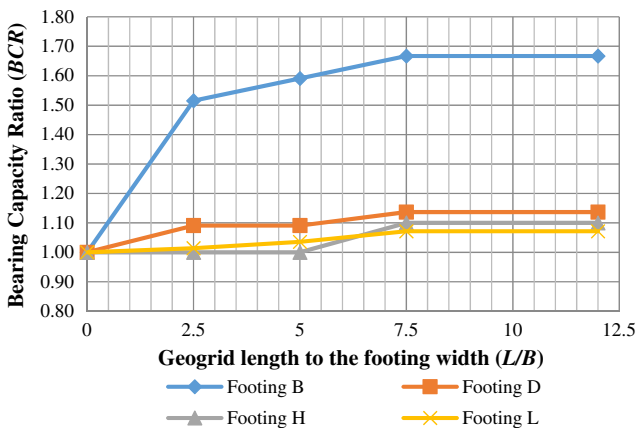

Fig. 16 Relationship of bearing capacity ratio *BCR* vs geogrid extension (L/B) for footings (B), (D), (H), and (L)

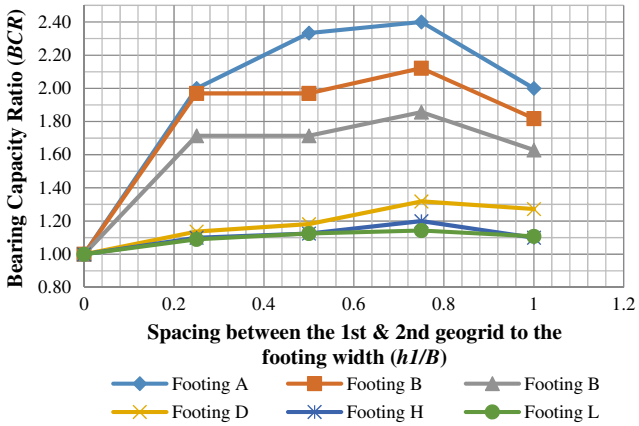

Fig. 17 Relationship of bearing capacity ratio (BCR) vs first and second geogrid spacing (*h1/B*) for footings (A), (B), (C), (D), (H), and (L)

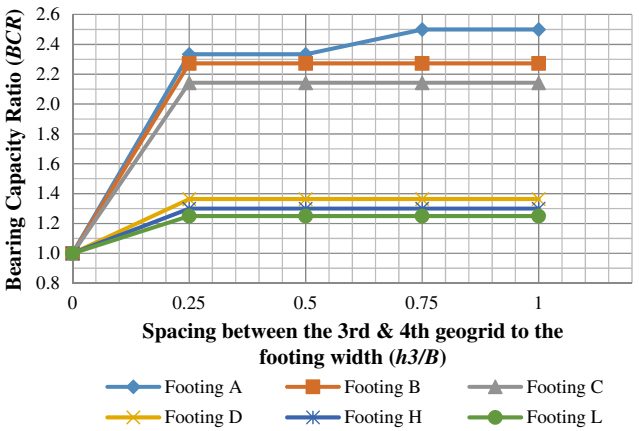

Fig. 19 Relationship of bearing capacity ratio(BCR) vs third and fourth geogrid spacing (*h3/B*) for footings (A), (B), (C), (D), (H), and (L)

proportion between footing width (*B*) and the improvement in the BCR that ranges between 25 and 150%, with the (*h2/b*) optimum value = 0.75 for all of the tested footings for three reinforcement layers. The same (BCR) improvements were traced as shown in Fig. 19, for the case of using four reinforcement layers. So there was no gain from using the fourth layer.

Settlement Figure 20 a and b illustrate the settlement (mm) for footings (A), (B), (C), (D), (H), and (L), respectively, in order to define the optimum value for h_2/B regarding their associated settlement values.

It can be concluded that $h2/B = 0.75$ had the least settlement; therefore, it was the optimum value.

Optimum number of geogrid layers A package of finite element models was carried out to assess the effect of number of geogrids on the mobilized BCR and the associated settlements. Figure 21 a and b represent both of BCR and settlement (mm) vs number of geogrids (*N*) for footings (A), (B), and (C). The inspection of the results revealed that the BCR value rises with the increase of geogrid layers up to $N = 3$ but the settlement (mm) for $N = 4$ and 5 is less than the settlement for $N = 3$, with minor reduction in settlement for the fifth geogrid layer. The same results were observed for the finite element models of the footings (D), (H), and (L), as shown in Fig. 22a, b.

So, it can be concluded that for the settlement considerations, the optimum number of geogrid reinforcement layers

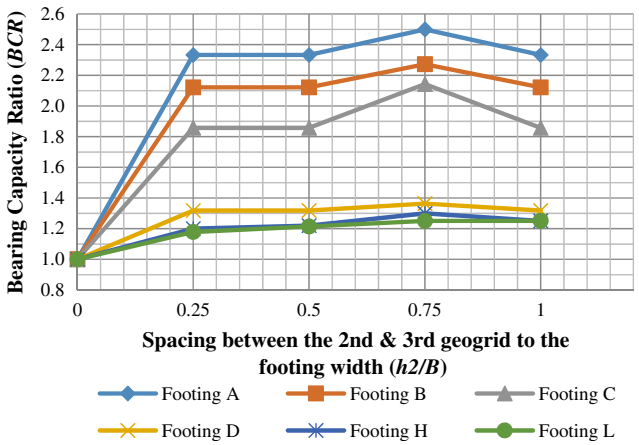

Fig. 18 Relationship of bearing capacity ratio(BCR) vs second and third geogrid spacing (*h2/B*) for footings (A), (B), (C), (D), (H), and (L)

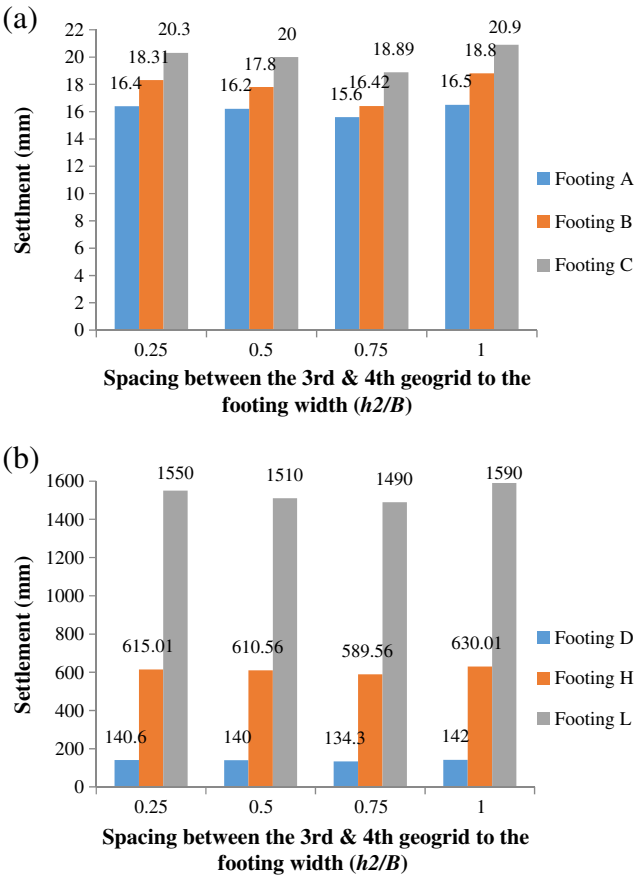

Fig. 20 Relation of footing settlement (mm) vs. second and third geogrid spacing (*h2/B*) for footings **a** (A), (B), and (C), and **b** (D), (H), and (L)

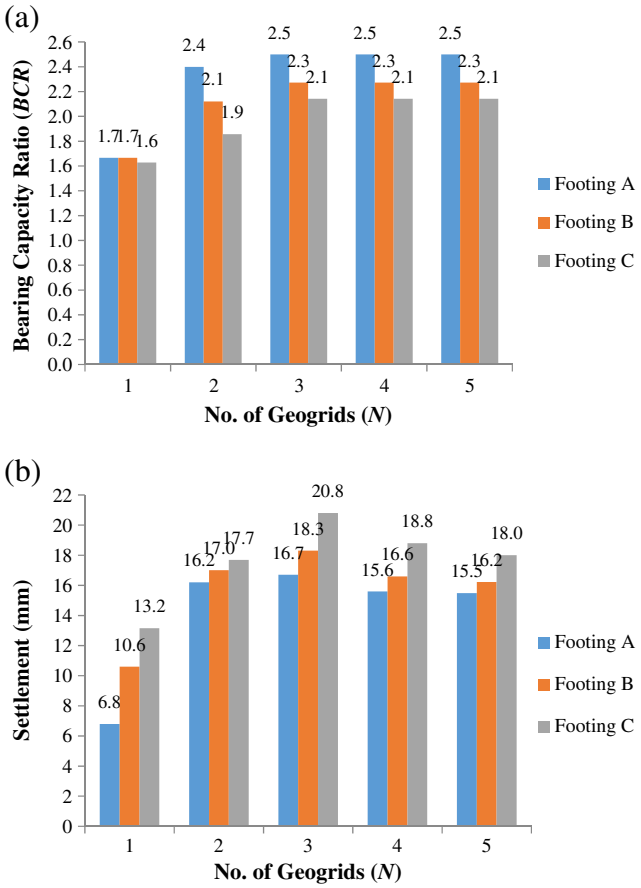

Fig. 21 Effect of number of geogrid layers (*N*) for footings (A), (B), and (C) on **a** bearing capacity ratio (BCR) and **b** footing settlement

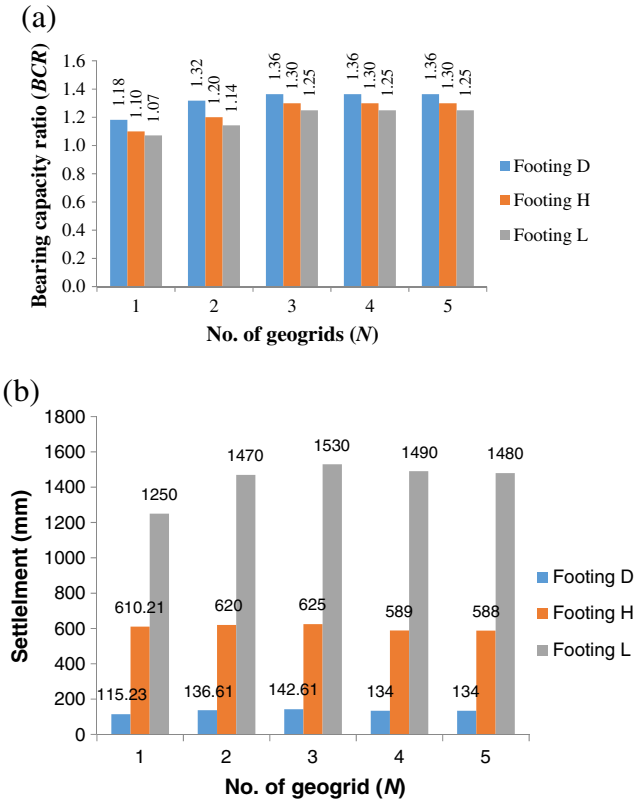

Fig. 22 Effect of number of geogrid layers (*N*) for footings (D), (H), and (L) on **a** bearing capacity ratio (BCR) and **b** footing settlement

under rigid strip footing overlaying a reinforced sand dunes is four layers.

Conclusions

A series of numerical model tests was carried out to assess the behavior of a rigid strip footing founded on unreinforced and reinforced sand dunes in terms of BCR and settlement. The research aimed to define the optimum parameters influencing the (footing-sand dune-geogrid) system, the embedment depth for the first and successive geogrid reinforcement layers (*u/B* and *h/B*), the extension of the reinforcement under the footing relative to its width (*L/B*), and the optimum number of geogrid reinforcement (*N*). Based on the numerical model test results, the following conclusions may be drawn:

1. As comparing the output of the proposed numerical model test results with those of the previously studied experimental model, an acceptable agreement was traced for the behavior pattern and the critical values of the geogrid parameters.
2. The numerical modeling output proved that the placement of the geogrid reinforcement layer/s at the proper place inside the sand dunes body caused a respectable enhancement in the mobilized bearing capacity with a decrease in settlements in the reinforced soil supporting the strip footing.
3. The ideal first geogrid burial expressed as (*u/B*) that mobilizes the maximum ultimate bearing capacity of the (dune sand-geogrid) composite was about 0.25 times the footing width, which shows an acceptable agreement with that of Shukla and Mohyeddin 2017 (0.2 *B*).
4. The optimum vertical spacing of each two successive layers of geogrids in terms of (*h/B*) that activates the maximum ultimate bearing capacity of (dune sand-geogrid) composite was about 0.75 times the footing width.
5. The most favorable geogrid length beneath the strip footing in terms of (*L/B*) that mobilizes the maximum ultimate bearing capacity of the (dune sand-geogrid) composite bed was about 7.5 times the footing width.
6. The optimum number of geogrid layers below strip footing is three layers for the bearing capacity considerations and four layers for the settlement considerations.
7. The study showed a direct proportional relation between the number of reinforcement layer and the BCR and an inverse proportional relation between the footing width and the mobilized BCR.

Acknowledgments The authors like to express their appreciations to Eng. Ahmed Gamal for carrying out the experiments related to this paper and to Dr. Ashraf El-Ashaal as a member of the super vision team. Grateful thanks for Construction and Building (CB) Department, AASTMT, Cairo branch, and Structures Research Institute, Ministry of Irrigation, Egypt, for providing a helpful support upon the implementation of experimental phase of this research.

References

Adams MT, Collin JG (1997) Large model spread footing load tests on geosynthetics reinforced soil foundations. J Geotech Geoenviron 123(1):66–72

Akinmusuru JO, Akinbolade JA (1981) Stability of loaded footings on reinforced soil. J Geotech Eng Div ASCE 107(6):819–827

Alamshahi S, Hataf N (2009) Bearing capacity of strip footings on sand slopes reinforced with geogrid and grid-anchor. Geotext Geomembr 27:217–226

Al-Sinaidi AR, Ali A. H. (2006) Improvement in bearing capacity of soil by geogrid-an experimental approach, IAEG2006, United Kingdom

Aria S, Shukla SK, Mohyeddin A (2017) Optimum burial depth of geosynthetic reinforcement within sand bed based on numerical investigation. Int J Geotech Eng. https://doi.org/10.1080/19386362.2017.1404202

Asakereh A, Tafreshi SM, Ghazavi M (2012) Strip footing behavior on reinforced sand with void subjected to repeated loading. International Journal of Civil Engineering 10:139–152

Basudhar PK, Saha S, Deb K (2007) Circular footings resting on geotextile-reinforced sand bed. Geotextiles and Geomembranes 25(6):377–384

Boushehrian JH, Hataf N (2003) Experimental and numerical investigation of the bearing capacity of model circular and ring footings on reinforced sand. Geotextiles and Geomembranes 23(2):144–173

Chao SJ (2006) Study of geosynthetic reinforced subgrade expressway in Taiwan. Fourth International Conference on Soft Soil Engineering (4th ICSSE), Vancouver, Canada: 237-243.

Chao SJ (2008) Performance study on geosynthetic reinforced shallow foundations. Sixth International Conference on Case Histories in Geotechnical Engineering, Arlington, VA.: 7.35a.

El Sawwaf MA (2007) Behavior of strip footing on geogrid-reinforced sand over a soft clay slope. Geotext Geomembr 25(1):50–60

Fragaszy RJ, Lawton E (1984) Bearing capacity of reinforced sand subgrades. J Geotech Eng Div ASCE 110(10):1500–1507

Ghazavi M, Lavasan AA (2008) Interference effect of shallow foundations constructed on sand reinforced with geosynthetics. Geotext Geomembr 26(5):404–415

Ghosh A, Bera AK (2005) Bearing capacity of square footing on pond ash reinforced with jute-geotextile. Geotext Geomembr 23(2):144–173

Giroud JP, Noiray L (1981) Geotextile-reinforced unpaved road design. J Geotech Eng Div 107(9):1233–1254

Guido VA, Chang DK, Sweeney MA (1986) Comparison of geogrid and geotextile reinforced earth slabs. Can Geotech J 23:435–440

Hegde A, Sitharam TG (2015) 3-Dimensional numerical modelling of geo-cell reinforced sand beds. Geotext Geomembr 43:171–181

Holtz RD, Christopher BR, Berg RR (1997) Geosynthetic engineering. Bitech Publishers Ltd., Canada

Hussein MG, Meguid MA (2016) A three-dimensional finite element approach for modeling biaxial geogrid with application to geogrid-reinforced soils. Geotext Geomembr 44:295–307

Khing KH, Das BM, Puri VK, Cook EE, Yen SC (1993) The bearing capacity of a strip oundation on geogrid reinforced sand. Geotext Geomembr 12:351–361

Madhavi, G. and, Somwanshi, A. (2009) Effect of reinforcement form on the bearing capacity of square footings on sand, Geotext Geomembr vol. 27, pp. 409–422.

Mosallanezhad M, Taghavi SH, Hataf N, Alfaro MC (2016) Experimental and numerical studies of the performance of the new reinforcement system under pull-out conditions. Geotext Geomembr 44:70–80

Omar MT, Das BM, Puri VK, Yen SC (1993) Ultimate bearing capacity of shallow foundations on sand with geogrid reinforcement. Journal of Canadian Geotechnical 30:545–549

Patra CR, Das BM, Atalar C (2005) Bearing capacity of embedded strip foundation on geogrid-reinforced sand. Geotext Geomembr 23: 454–462

Pinto MI (2002) Applications of geosynthetics for soil reinforcement. Proc. 4 th Int. Conference on Ground Improvement Techniques, Malaysia, 147-162.

Sakti JP, Das BM (1987) Model tests for strip foundation on clay reinforced with geotextile layers. Transp Res Board 1153:40–45

Sharma, R, Chen, O., Abu-Farsak, M. and Yoon, S. (2009) Analytical modeling of geogrid reinforced soil foundation, Geotext Geomembr vol. 27, pp. 63–72 .

Shukla SK, Chandra S (1994a) A generalized mechanical model for geosynthetic-reinforced foundation soil. Geotext Geomembr 13:813–825

Shukla SK, Chandra S (1994b) A study of settlement response of a geosynthetic- reinforced compressible granular fill-soft soil system. Geotext Geomembr 13:627–639

Shukla, S.K., Sivakugan, N. and Das,B. (2011) A state-of-the-art review of geosynthetic-reinforced slopes, Int J Geotech Eng, 5:1, 17-32, DOI: https://doi.org/10.3328/IJGE.2011.05.01.17-32

Wu LL (2003) Design and performance analysis of geosynthetic applications in railroad track mitigation, Ph. D. Dissertation, National Cheng-Kung University, Taiwan.

Yetimoglu T, Wu JTH, Saglamer A (1994) Bearing capacity of rectangular footings on geogrid-reinforced sand. J Geotech Eng ASCE 120: 2083

Yu Y, Damians IP, Bathurst RJ (2015) Influence of choice of FLAC and PLAXIS interface models on reinforced soil–structure interactions. Comput Geotech 65:164–174

Zidan A (2012) Numerical study of behavior of circular footing on geogrid-reinforced sand under static and dynamic loading. Geotech Geol Eng 30:499–510